Chain aggregate structure and magnetic birefringence in polydisperse ferrofluids

Alexey O. Ivanov* and Sofia S. Kantorovich†
Department of Mathematical Physics, The Urals State University, 51 Lenin Avenue, Ekaterinburg 620083, Russia
(Received 9 September 2003; published 9 August 2004)

The theory of particle association in chains in dilute ferrofluids and dipole fluids is generalized to the case of polydisperse systems. The chains could be formed by ferroparticles of different sizes, so various types of chain aggregates are considered. The probabilities of chain structure appearance are calculated, and the phase diagram, allowing to find the most probable structure with only the continuous particle size distribution known, is built. Our results demonstrate that in spite of a very weak dipole-dipole interaction between the small size fraction particles, their presence exerts a decisive influence on the ferrofluid microstructure. The chain shortening caused by the small particles sticking to the edges of chains formed by large particles is discovered theoretically. The latter effect is proved to exist by the recent computer simulations on bidisperse ferrofluid makeup. The application of the developed model to the description of magnetic birefringence phenomena in weak external magnetic fields shows a very good agreement with experimental data.

DOI: 10.1103/PhysRevE.70.021401 PACS number(s): 82.70.−y, 61.20.Gy, 75.50.Mm, 78.20.Ls

I. INTRODUCTION

The materials, the properties of which could be effectively controlled by an external magnetic field, are of great interest either from theoretical or practical points of view. Magnetic fluids (ferrofluids, ferrocolloids) are the suspensions of magnetic nanosized particles (Fe oxides, Co, Ni, etc.) covered by a solvent layer. The magnetic particles generally are approximately 10 nm in diameter. Particles of this size, whether they be ferrite or metal, possess a single magnetic domain only. So, each particle has its own magnetic moment m, the value of which is proportional to the magnetic core volume and depends upon the saturation magnetization of the material M_0: $m = M_0 \pi x^3/6$; here x stands for the particle magnetic core diameter. So, particles are involved not only into the Brownian motion, but also interact with each other forming different aggregates. Rheological, hydrodynamic, diffusion, magnetic, and optical properties of a ferrofluid change by hundred times under an applied magnetic field of moderate strength (less than 40 kA/m). So, such material is a challenging subject for scientific research as well as for different applications.

Recent computer simulations [1–4] have shown the microscopic structure of dipolar model fluids to be much more complex than previously expected. The system at a high dipolar strength and low volume fraction has proved to associate in chain aggregates [2–4], while at higher volume fraction a spontaneous formation of ferroelectric phase has been observed [1]. An additional attractive force presence has resulted in a usual condensation, as in the Stockmayer fluid [3].

It is well known, that magnetic fluids become optically anisotropic [5–10] and demonstrate an abrupt viscosity increase [11] when subjected to a magnetic field. These phenomena explanations in terms of chain aggregates seem to be the most commonly used one. A lot of experimental studies, demonstrating not only the chain-like aggregate existence but also their great influence upon diffusional and hydrodynamic properties of ferrofluids, are worth mentioning (see, for example, Ref. [12]). The condensation of ferroparticles, known as the phase separation, has also been observed [13].

The peculiar feature of ferrofluids is the interparticle magnetic dipole-dipole interaction. This interaction has a noncentral character and depends not only on the distance between ferroparticle centers but also on the mutual orientation of their magnetic moments. Hence, the chain aggregates composed of ferroparticles, the magnetic moments of which are in the most favorable energetic "head-to-tail" position, prove to be typical for magnetic fluids. So, the computer simulations and experimental observations were accompanied by theoretical studies of the chain formation process [14–16]. Two approaches for the chain aggregate description were proposed. The first one used so-called dynamic method [14], i.e., particle combination/recombination processes in chains were treated as reversible chemical reactions. With the dynamic equilibrium in demand the chain distribution as well as other important properties of the system could be obtained. The second commonly used approach was based on the free energy minimization (see Ref. [16]). The free energy was regarded as a functional of the chain distribution density. So, this method was called the density functional approach. The equivalence of these methods is an evident consequence of the thermodynamic fundamentals. According to these works, a considerable part of ferroparticles at low densities and intensive magnetic dipole interaction is connected in chains, the mean length of which appears to be an increasing function of a ferroparticle concentration. Naturally, an external magnetic field stimulates the chain formation. Unfortunately, no theoretical model properly describing the magnetic field influence upon the chain formation process has been built yet. Moreover, almost all known computer simulations and theoretical studies deal with model monodisperse dipolar fluids and magnetic colloids.

The point is that such a monodisperse approximation does neglect an extremely important and undoubtedly inherent feature of real ferrofluids, that is the polydispersity. There is only one theoretical work [17] where an attempt to allow for

*Email address: alexey.ivanov@usu.ru
†Email address: sue.kantorovich@usu.ru

the polydispersity influence on the chain formation has been made. In this paper the real magnetic fluid is approximated by a model bidisperse system, containing a small number of large particles and a great amount of small ones. Still, in this model only large particles can form aggregates, while small particles remain just an environment. Computer simulations of the bidisperse model ferrofluid have been done [4] as well. The results of this investigation will be discussed later.

This paper addresses the basic question of the ferrofluid polydispersity influence on the chain aggregate structure. It is when the theoretical model, describing the different size particle aggregation in chains, is successfully developed and the mathematical algorithm, allowing to account for all chains having different topological structures, is worked out (Sec. II). As the peculiarities, brought by the polydispersity into the chain formation process, become apparent even in an example of a two-fraction system, we focus our attention on the following approach. The real polydisperse ferrofluid is approximated by the bidisperse system consisting of small and large particle fractions. The free energy density functional for this bifractional system is built on the basis of the monodisperse one (Sec. III). An effect of large particle chain shortening caused by the small particle presence has been found and compared with the same effect described in Ref. [4] (Sec. IV). The relative shortening is close to the one found during computer simulations. The probabilities of chain structure existence are studied, and a phase diagram of aggregated ferrofluid is built. One of the main results is the following: the majority of large particles in the real polydisperse ferrofluid is connected in short chains, and the most probable structure is a chain consisting of some large particles, at both edges of which there is one small particle. The model check-up is carried out in Sec. V. The chain distribution obtained is used for a description of the experimentally observed magnetic birefringence in a weak field limit. In this case the optical anisotropy is assumed to be caused by the chain orientation only. Theoretical results prove to be close to those of the experiment. The main summary is given in Sec. VI.

II. BIDISPERSE MODEL: THE ALGORITHM

Let us regard a model bidisperse system consisting of two fractions: the small particles form the first fraction and the large ones form the second fraction. To use the energy density functional method the following assumptions are traditionally adopted: (a) Each fraction consists of identical spherical particles with the constant magnetic moment; (b) Structures that differ from those of chains are ignored; (c) Only the interaction between the nearest neighboring particles in every chain is taken into account; and (d) The diluted ferrofluids are studied, that is why, an interaction between chains is not considered. Thus, it is necessary to obtain the free energy functional for such a system, using the expression of the partition function. The final problem is to find the minimum of the free energy as a functional of the chain distribution under the mass balance condition.

To obtain the free energy functional for such a bifractional system, one needs to find the energies of all topologically

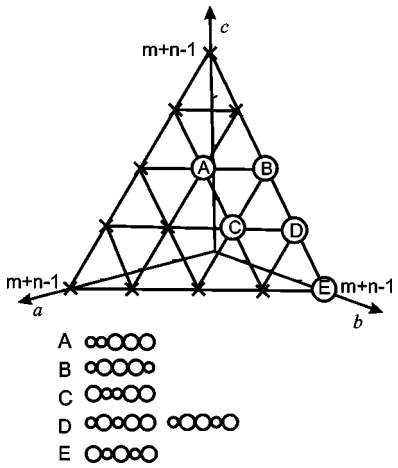

FIG. 1. Equation (1) integer solution surface for chains containing three large and two small particles. Those solutions that correspond to the real chain structures are encircled (A)–(E).

different chains, consisting of n large particles and m small ones. The algorithm, allowing to account for all chains being distinguishable not only from the energetic but also from the entropic point of view, is as follows [18]. For each chain its free energy is uniquely determined by the following six parameters: $e_{11},e_{12},e_{22},a,b,c$. Here, e_{11},e_{12},e_{22} are the effective interaction energies between two nearest neighboring particles from corresponding fractions 1 and 2, for example, e_{12} is the energy of the small and large interparticle bond. The values of a,b,c are the numbers of e_{11},e_{12},e_{22} bonds, respectively. Let us introduce two vectors: the energy vector $\mathbf{E}=(e_{11},e_{12},e_{22})$ and the structure vector $\mathbf{S}=(a,b,c)$. Their scalar product $\mathbf{S}\cdot\mathbf{E}=ae_{11}+be_{12}+ce_{22}$ equals to the effective chain energy. It should be stressed, two chains with the same energy are not always entropically indistinguishable, see Fig. 1, structure D. As the numbers a,b,c stand for the quantity of bonds in a chain, there are some restrictions to be imposed.

(1)

$$a+b+c=m+n-1. \tag{1}$$

It means that the total number of bonds per chain $m+n-1$ equals to the sum of three different type bond numbers;

(2) $a,b,c\in\mathbf{N}$. The number of bonds is to be natural. In Fig. 1 the plane of all natural-valued solutions of Eq. (1) is built for $m=2,n=3$, for example;

(3) $a\leqslant m-1$. It means that the $1-1$ bond number cannot be larger than the number of small particles minus one; $c\leqslant n-1$. This is the similar restriction on the $2-2$ bond number.

Restrictions on the $1-2$ bond number are a bit more cumbersome: if $m<n$ then $b\leqslant 2m$; if $n<m$ then $b\leqslant 2n$; if $m=n$ then $b\leqslant 2m-1$. The maximal number of $1-2$ bond could be reached in a chain, where particles from each fraction are alternated with each other. Thus, this number is limited by the quantity of that very particles which are in minority in a chain. For example, for a chain consisting of 2 small and 3 large particles (Fig. 1) the maximal value of b equals to $4=2m,m=2$ and is reached in the structure E.

(4) $m<n+1\Rightarrow c>0,n<m+1\Rightarrow a>0$. This provides at

least one direct 1−1 or 2−2 contact if the numbers of various fraction particles in a chain differ for more than unity; $(n\neq 0)\&(m\neq 0)\Rightarrow b>0$. To put it differently, if a chain contains particles of both fractions, the 1−2 contact is inescapable.

Those solutions that correspond to the real chain structures are encircled (Fig. 1). As a result, the algorithm consists of two steps: (a) to find all natural-valued solutions of equation (1); (b) to choose those solutions that meet real chain structures, i.e., to impose the earlier listed restrictions. And what is more, such a vector solution uniquely defines the chain structure class. Thus, for each pair of $m,n: m+n\geqslant 1$ a finite number of energetically distinguishable chain structures $I(n,m)$ exists, to each chain type an index $i\in[1,I(n,m)]$ is given. Of course, $I(n,m)$ grows with $n+m$ increase. The set $\{\mathbf{S_i}=(a_i,b_i,c_i)\}$ consists of structure vectors (energetic classes) for fixed n,m. The function $g(i,n,m)$ stands for the concentration of ith structure chains, containing n large and m small particles. As it was noted before not all of the chains having the same energy are entropically indistinguishable. For example, for the class D (see Fig. 1) we have two entropically distinguishable structures. Thus, to allow for all entropically (topologically) different chains belonging to the same energy class it is essential to introduce a factor, the value of which equals to such subclasses quantity. So, let us define an entropy factor $K(i,n,m)$ denoting a number of topologically different chain structures relevant to the same energetic class S_i, for example, $K(i_D,3,2)=2$ for D class in Fig. 1. There is no general formula to describe $K(i,n,m)$. Some entropy factors for different topological classes could be found in expression (11).

The worked out algorithm could be generalized for any finite number of fractions. It is just a question of the dimension of a hyperplane defined by Eq. (1).

III. BIDISPERSE MODEL: THE FUNCTIONAL

The density functional approach used for monodisperse systems in Ref. [16] drives to the following target setting:

$$F=kT\sum_{n=1}^{\infty}g(n)\left[\ln\frac{g(n)}{\mathrm{e}}-\ln Z_n\right]. \tag{2}$$

Here $g(n)$ stands for a concentration of chains containing n particles per unit volume; kT is the thermal energy, and Z_n has a meaning of a chain partition function

$$Z_n=\int\prod_{i=1}^{n-1}d\mathbf{r}_{\mathbf{i}\ \mathbf{i+1}}\int\prod_{i=1}^{n}d\mathbf{\Omega}_{\mathbf{i}}\times\exp\left[-\sum_{i=1}^{n-1}\frac{U_d(i\ i+1)+U_s(i\ i+1)}{kT}\right],$$

$$U_d(i\ i+1)=-\left[3\frac{\langle\mathbf{m_i}\cdot\mathbf{r}_{\mathbf{i}\ \mathbf{i+1}}\rangle\langle\mathbf{m_{i+1}}\cdot\mathbf{r}_{\mathbf{i}\ \mathbf{i+1}}\rangle}{r_{i\ i+1}^5}-\frac{\langle\mathbf{m_i}\cdot\mathbf{m_{i+1}}\rangle}{r_{i\ i+1}^3}\right],$$

$$\mathbf{r}_{\mathbf{i}\ \mathbf{i+1}}=\mathbf{r_{i+1}}-\mathbf{r_i},$$

$$d\mathbf{\Omega}_{\mathbf{i}}=(4\pi)^{-1}\sin\omega_i d\omega_i d\zeta_i, \tag{3}$$

$$d\mathbf{r}_{\mathbf{i}\ \mathbf{i+1}}=r_{i\ i+1}^2 dr_{i\ i+1}\sin\theta_{i\ i+1}d\theta_{i\ i+1}d\varphi_{i\ i+1},$$

where the vector $\mathbf{r}_{\mathbf{i}\ \mathbf{i+1}}(r_{i\ i+1};\theta_{i\ i+1};\varphi_{i\ i+1})$ connects the centers of ith and $i+1$th particles $(i=1,2,\ldots,n-1)$, the vector $\mathbf{\Omega_i}(\omega_i;\zeta_i)$ determines the ith particle magnetic moment direction $(\mathbf{m_i}=m\mathbf{\Omega_i})$; $U_d(i\ i+1)$ denotes the magnetic dipole-dipole interaction potential between two nearest neighboring particles in a chain; as far as the potential $U_s(i\ i+1)$ is concerned, it stands for a central interparticle interaction (steric repulsion, van der Waals attraction, electrostatic repulsion in ionic stabilized ferrofluids). Usually the hard sphere potential is used: $U_s=U_{\mathrm{HS}}$. In cases of the zero and the infinite external magnetic field $\mathbf{H}$, all of the factors in products $\Pi_{i=1}^{n-1}d\mathbf{r}_{\mathbf{i}\ \mathbf{i+1}}$, $\Pi_{i=1}^{n}d\mathbf{\Omega_i}$ have the same value and so the factorization of expression (3) takes place, i.e., the chain partition function Z_n could be presented in the form

$$\ln Z_n=\ln v^{n-1}+(n-1)e,$$

$$e=\ln\left\{\frac{1}{v}\int d\mathbf{r}_{12}\int d\mathbf{\Omega}_2\exp\left[-\frac{U_d(12)+U_s(12)}{kT}\right]\right\}. \tag{4}$$

The particle volume v plays a part of the normalizing coefficient. The parameter e denotes an effective energy of one interparticle bond. Its calculation could be found in Refs. [14,15]. For zero and infinite fields, for example, these energies are

$$e(H=0)=\ln\left[\frac{\exp(2\gamma)}{3\gamma^3}\right],\quad e(H\to\infty)=\ln\left[\frac{\exp(2\gamma)}{3\gamma^2}\right], \tag{5}$$

$$\gamma=\frac{\pi m^2}{6vkT}.$$

Here γ stands for the dipole-dipole coupling constant. It is clearly seen that the effective energy of the interparticle bond in the case of an infinitely intensive magnetic field is larger than in a zero field, the difference is equal to $\ln\gamma$. Thus, in magnetic saturation the chain length becomes larger on average. Unfortunately, the precise equilibrium chain lengthening in a field of moderate strength appears to be much more complicated mathematical problem, the solution of which has not been found yet. It is caused by the absence of factorization in the partition function (3), because the interaction between the particle magnetic moments and an external field leads to the interparticle orientational correlations between all the particles in a chain. The field orientation of the stiff rod-like chain aggregates is the only known approach to take the magnetic field influence into account (see Ref. [17]). On the other hand, the mean chain length in equilibrium is a monotonously increasing function of an external field strength by all means. That is why, the study of two limiting cases (field absence and saturation condition) provides a physically adequate description of the equilibrium chain formation.

For a bifractional system the following free energy functional appears as a natural generalization of the traditional density functional approach [2–4]:

$$F = kT \sum_{i,n,m} g(i,n,m)\left[\ln\frac{g(i,n,m)}{\mathrm{e}} - \ln Z_{i,n,m}\right],$$

$$\ln Z_{i,n,m} = \ln v_1^a v_{12}^b v_2^c + \mathbf{E}\cdot\mathbf{S_i}, \quad v_{12} = (v_1^{1/3} + v_2^{1/3})^3/8, \quad (6)$$

where v_1, v_2 are the first and the second fraction particle volumes. The generalization of expressions (5) leads to the fact that the energy vector components $\mathbf{E} = (e_{11}, e_{12}, e_{22})$ are the functions of corresponding dipole-dipole coupling constants. The summation here (6) is carried out taking into account all entropically and energetically distinguishable chains. So, this sum contains the equal terms relevant to the different entropic classes for each energetic one. To avoid it, the entropic factor $K(i,n,m)$ introduced earlier is used. Thus, finally the following target setting (7) for a bidisperse model is obtained

$$F = kT \sum_{n+m\geq 1}^{\infty} \sum_{i=1}^{I(n,m)} K(i,n,m) g(i,n,m) \times \left[\ln\frac{g(i,n,m)v(i,n,m)}{\mathrm{e}} - \mathbf{E}\cdot\mathbf{S_i}\right],$$

$$v(i,n,m) = v_1^{-a} v_{12}^{m-b} v_2^{n-c}. \quad (7)$$

Here F stands for the free energy volume density of the system containing different chains formed by particles from both fractions. The first term in the sum (7) corresponds to a chain mixture ideal gas, while the second one allows for the interactions. There are two differences between the functionals in the monodisperse and our cases. The first one is the combinatorial factor $K(i,n,m)$. The scalar product $\mathbf{E}\cdot\mathbf{S_i}$, describing all possible interparticle bonds in each chain, is the second one. Finally, the free energy (7) minimum has to be found under the mass balance conditions

$$\frac{\rho_1}{v_1} = \sum_{n+m\geq 1}^{\infty} \sum_{i=1}^{I(n,m)} K(i,n,m) g(i,n,m) m, \quad (8)$$

$$\frac{\rho_2}{v_2} = \sum_{n+m\geq 1}^{\infty} \sum_{i=1}^{I(n,m)} K(i,n,m) g(i,n,m) n, \quad (9)$$

where ρ_1, ρ_2 are the volume concentrations of small and large particle fractions, respectively. Using the Lagrange method the solution obtained is

$$g(i,n,m) = \exp[\lambda_1 m + \lambda_2 n + \mathbf{E}\cdot\mathbf{S_i}]/v(i,n,m), \quad (10)$$

and λ_1, λ_2 are the Lagrange multipliers to be calculated from Eqs. (8) and (9). This problem is solvable only numerically. However, it is useful to perform analytical calculations of the different chain class contribution. First, we sum up the large particle chains, then the chains with one small particle at the edge, then the large particle chains with two small particles attached to both edges, etc. Such a regrouping turns the sums (8) and (9) into the fast decreasing series composed by analytical functions of parameters λ_1, λ_2.

The examples of classes with corresponding concentrations and entropic factors are given later to illustrate the procedure

$$\begin{gathered}
g(\mathrm{I},n,0) = \exp(-e_{22}) p_2^n / v_2, \quad K(\mathrm{I},n,0) = 1, \\
g(\mathrm{II},n,1) = \exp(-e_{22}) p_1 p_2^n / v_2, \quad K(\mathrm{II},n,1) = 1, \\
g(\mathrm{III},n,2) = \exp(-e_{22}) p_1^2 p_2^n / v_2, \quad K(\mathrm{III},n,2) = 1, \\
g(\mathrm{IV},n,1) = \exp(-e_{22}) p_1 p_2^n \exp(e_{12}-e_{22})(v_{12}/v_2^2), \\
K(\mathrm{IV},n,1) = n/2, \quad n = 2j, \quad K(\mathrm{IV},n,1) = (n-1)/2, \\
n = 2j+1, \\
g(\mathrm{V},n,2) = \exp(-e_{22}) p_1^2 p_2^n \exp(e_{12}-e_{22})(v_{12}/v_2^2), \\
K(\mathrm{V},n,2) = n/2, \quad n = 2j, \quad K(\mathrm{V},n,2) = (n-1)/2, \\
n = 2j+1, \\
g(\mathrm{VI},n,2) = \exp(-e_{22}) p_1^2 p_2^n \exp[2(e_{12}-e_{22})](v_{12}^2/v_2^3), \\
K(\mathrm{VI},n,2) = n(n-2)/4, \quad n = 2j, \\
K(\mathrm{VI},n,2) = (n-1)^2/4, \quad n = 2j+1, \\
g(\mathrm{VII},n,2) = \exp(-e_{22}) p_1^2 p_2^n \exp(e_{11}-e_{22})(v_1/v_2^2), \\
K(\mathrm{VII},n,2) = n/2, \quad n = 2j, \quad K(\mathrm{VII},n,2) = (n-1)/2, \\
n = 2j+1, \\
g(\mathrm{VIII},n,2) = \exp(-e_{22}) p_1^2 p_2^n \exp(e_{11}-e_{12})(v_1/v_2 v_{12}), \\
K(\mathrm{VIII},n,2) = 1, \\
p_1 = \exp(\lambda_1 + e_{12}), \quad p_2 = \exp(\lambda_2 + e_{22}).
\end{gathered} \quad (11)$$

The geometrical presentation of these classes is given in Fig. 2. Such a presentation is not only convenient for the series summation but also drives us to an important recurrence: parameters p_1, p_2 are in powers of the corresponding fraction particle numbers for each chain. As for the exponential powers, they appear due to one to another bond changes. For the transition from the IInd to the IVth class, one small particle from the edge is removed inside the chain between two large particles, thus, destroying one 2–2 bond and one 1–2 bond and replacing them by two 1–2 bonds. The energy difference appears in an exponent power.

"What is the right number of classes to be taken into account for a proper description of the free energy?"—that is the question. It is quite clear that the value of $g(i,n,m)$ depends upon the interaction energies e_{11}, e_{12}, e_{22} and the volume concentrations ρ_1, ρ_2. So, to answer the latter question it is essential to deal with real ferrofluids.

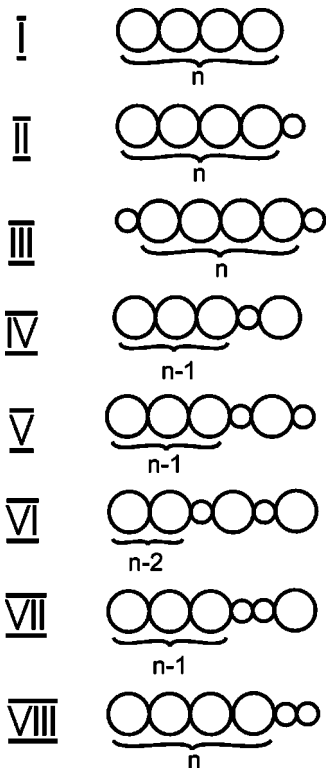

FIG. 2. Energetic classes. Chain aggregates are composed by n large particles and zero (class I), one (classes II and IV), and two small particles (classes III, V–VIII) with concentrations and entropy factors given in expression (11).

IV. REAL FERROFLUIDS: RESULTS AND DISCUSSIONS

The particle size distribution in real ferrofluids is continuous, so it is necessary to build an appropriate bidisperse approximation. The method of obtaining a model bidisperse distribution was discussed in Ref. [19]. It is based on the condition of coincidence between experimental and model magnetization curves. In Table I the model bidisperse distribution of three real ferrofluids could be found (samples A,B,D). The main fractions (mole portion $\varphi_1 \sim 90\% - 95\%$) consist of small particles with magnetic core diameter $x_1 \sim 7-9$ nm and constant magnetic m_1. The second fractions consist of small number (mole portion $\varphi_2 \sim 5\% - 10\%$) of large particles ($x_2 \sim 15-18$ nm) with magnetic moment m_2. The solvent layer thickness l has the order of value $l \sim 2$ nm. So, the particle volumes are calculated as $v_i = \pi(x_i + 2l)^3/6$. The expressions for the effective energies e_{ij} as increasing functions of the interparticle dipole-dipole coupling constants are taken from Refs. [14,15] [expression (5)]. The energy values under an infinite magnetic field are usually $15\% - 20\%$ larger than the corresponding values in a field absence. Hence, the main fractions consist of particles with the negligibly weak interparticle attraction, whereas the interaction between large particles is quite intensive. Since, the energy e_{11} is extremely low, the 1–1 bond cannot be treated as a stable one. So, it is reasonable to exclude from the consideration all chain structures containing at least two small particles connected with each other (classes VII and VIII).

Under these assumptions the first three chain classes [see expression (11) and Fig. 2] turned out to be prevalent. The Ist class chains consist of n large particles only. Class II derives from the Ist one by adding one small particle to the chain edge. Chains, consisting of large particles in the middle, at both edges of which there is one small particle, form the IIIrd class. The contribution of chain classes with small particles between large ones (such as classes IV–VI in Fig. 2) into sums (8) and (9) turns out to be negligible. This fact is not an artificial consequence from the assumption of the nearest neighbor interaction. At the first sight, the latter approximation seems to be too rough to describe the situation when a small particle is sandwiched between two large ones (see classes IV–VI). However, if one compares the upper estimates of the Ist and the IVth chain class energies the following expressions could be obtained:

(1) nearest neighbors

$$I(n \text{ large particles}, 0 \text{ small particles}):$$

$$2\gamma_{22}(n-1),$$

$$IV(n-1 \text{ large particles}, 1 \text{ small particles}):$$

$$2\gamma_{22}(n-3) + 4\gamma_{12},$$

(2) first and second nearest neighbors

$$I(n \text{ large particles}, 0 \text{ small particles}):$$

$$2\gamma_{22}(n-1) + \gamma_{22}(n-2)/4,$$

$$IV(n-1 \text{ large particles}, 1 \text{ small particles}):$$

$$2\gamma_{22}(n-3) + 4\gamma_{12} + \gamma_{22}(n-4)/4 + 2\gamma_{22}[d_2/(2d_{12})]^3 + 2\gamma_{12}[d_{12}/(d_2+d_{12})]^3,$$

$$\gamma_{22} = m_2^2/kTd_2^3, \quad \gamma_{12} = m_1 m_2/kTd_{12}^3,$$

TABLE I. Bidisperse approximation for real ferrofluids (samples A, B, and D) and bidisperse system studied in computer simulations (sample C). For sample C $\rho_2 = 0.05$ and $\rho_1 = 0.0.1$.

Sample	x_1 (nm)	x_2 (nm)	φ_1	φ_2	ρ_m	e_{11}	e_{12}	e_{22}	Ref.
A	7.9	15.5	0.97	0.03	0.01	0.03	0.21	2.4	[8]
B	8.3	14.4	0.98	0.02	0.01	0.04	0.22	1.6	[8]
C	10.0	16.0				0.59	1.82	5.1	[4]
D	7.8	16.5	0.94	0.06	0.05	0.01	0.13	2.7	[19]

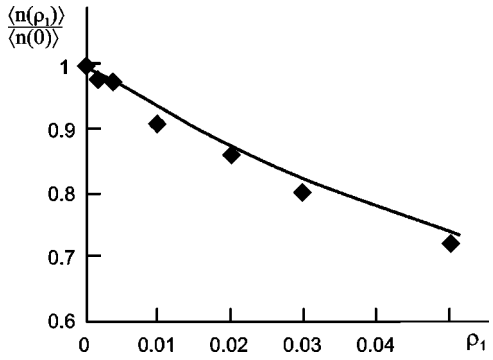

FIG. 3. Poisoning effect. The relative decrease of $\langle n \rangle$ (the mean number of large particle per chain) is plotted as a function of small particle volume concentration ρ_1. Points correspond to computer simulations (see Ref. [4]) (sample C, Table I), line describes the theoretical result.

$$d_2 = x_2 + 2l, \quad d_{12} = (x_1 + x_2)/2 + 2l.$$

Thus, the concentration of the Ist class chains related to the concentration of the IVth class chains is proportional to:

(1) nearest neighbors

$$g(I,n,0):g(IV,n-1,1) \sim \exp(4\gamma_{22} - 4\gamma_{12}) \gg 1,$$

(2) first and second nearest neighbors

$$g(I,n,0):g(IV,n-1,1) \sim \exp(4\gamma_{22} - 5\gamma_{12}) \gg 1.$$

Here we use the relations $x_2 \approx 2x_1, d_2 \approx 1.5 d_{12}$ which are typical for the bidisperse models of real commercial ferrofluids (see, for example, Table I). It means that chains from classes IV, V, etc., appear extremely rare. This result meets the conclusion in Ref. [4]: "… if a small particle is a member of a chain, it is predominantly attached to the end of the chain …."

It is worth mentioning that in Ref. [17] only large particle chains are taking into account. To check whether it is necessary to allow for the IInd and the IIIrd classes let us regard a model large particle fluid (ρ_2=const), with the small particle volume concentration ρ_1 scaling up. In this case, the larger is the small particle concentration the smaller is the mean number of large particles per chain $\langle n \rangle$. In other words, the presence of small particles drives to the chain shortening. This effect is caused by the appearance of chains from the IInd and the IIIrd energetic classes. A small particle sticking to the chain edge results in the "poisoning" of it, as the following chain length increase in this direction becomes energetically disadvantageous. Since the small particle concentration exceeds a value $\rho_1 \sim 10^{-2}$, the mean chain length $\langle n \rangle$ decreases sufficiently, in spite of the expected stimulation of chain aggregate formation due to the growth of total particle concentration. In Fig. 3 the relative chain length decrease is illustrated. The solid line (theoretical result) is quite close to the points which are taken from computer simulations [4]. The parameters of the latter model fluid are given in Table I, sample C.

After the poisoning effect is discovered, a natural question emerges: "How do the interparticle interaction energies influence upon the prevalence of chains from the one or another energetic class?" The answer is given by Fig. 4. The appearance probabilities for the chains of three main classes are given by the following ratio:

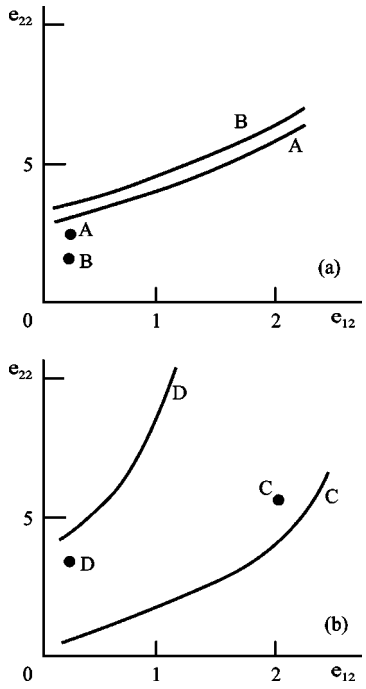

FIG. 4. Chain aggregate structure phase diagram for model bidisperse ferrofluids. The diagram is built in the plane of effective energies e_{12}, e_{22}. Curves and points A–D correspond to samples from Table I.

$$g(\mathrm{I},n,0):g(\mathrm{II},n-1,1):g(\mathrm{III},n-2,2) = 1:(p_2/p_1):(p_2/p_1)^2. \tag{12}$$

It should be stressed that the comparison of such probabilities is to be carried for the chains with the same total particle number in them only. As the parameters p_1, p_2 stand for the 1–2 and 2–2 bonds establishing probabilities, respectively, this expression becomes clear. Naturally, $p_1 = p_2$ equality means that the chains of these three classes are equiprobable. Consequently, the phase plane $Oe_{12}e_{22}$ presented in Fig. 4 is divided by the curve $p_1 = p_2$ into two regions of the chain structure predominance: above the curve there is an area of the Ist class chain structure domination, and below—the most probable are the chains from the IIIrd class. Thus, Figs. 4(a) and 4(b) have a meaning of the chain structure prevalence phase diagram for polydisperse ferrofluids. To use this phase diagram it is necessary to follow the algorithm:

(1) To obtain the parameters of a model bidisperse ferrofluid on the basis of known continuous particle size distribution for a real magnetic fluid;

(2) to calculate the volume concentrations of both fractions and the effective interaction energies e_{12}, e_{22} either influenced by an external magnetic field or not; and

(3) to determine the region in the phase diagram, which the point with just calculated coordinates belongs to.

The fact is, the region of parameters for any real ferrofluid is situated below the corresponding phase curve $p_1 = p_2$ [for

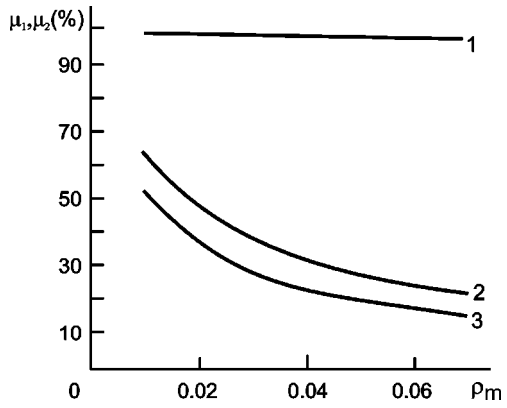

FIG. 5. Nonaggregated particles percentage μ_1 (curve 1) and μ_2 (curves 2 and 3) for both fractions is built for sample D (Table I) as a function of magnetic phase concentration ρ_m. The case of an external magnetic field absence is described by curve 2, while curve 3 represents the infinite field influence.

example, fluids A,B, Fig. 4(a); fluid D, Fig. 4(b)]. Thus, for commercial ferrofluids the most probable chain aggregates are those from the IIIrd class, consisting of several large particles, at both edges of which there is one small particle. Let us note, that the point of model fluid C from Table I is situated above the phase curve, see Fig. 4(b). It means that the main class in this fluid is the first one. This fact comes to an agreement with the result described in Ref. [4], where the mean number of small particles per chain is much less than unity.

It is worth mentioning, the mean chain length does not exceed 5–6 particles for various values of interaction energies e_{12}, e_{22} even under an infinite external magnetic field. Moreover, the higher concentration of chains in comparison with the monodisperse case is to be stressed. The dependencies μ_1 (curve 1), μ_2 (curves 2,3), which are the percentages of nonaggregated particles from both fractions, on the total magnetic phase concentration $\rho_m = \rho_1 x_1^3/(x_1+2l)^3 + \rho_2 x_2^3/(x_2+2l)^3$ are plotted in Fig. 5 for ferrofluid D (Table I). Curve 3 corresponds to the case of an infinite external magnetic field, curve 2—to its absence. As it could be seen, if $\rho_m \sim 0.05$, only some 10%–15% of large particles are nonaggregated. Small particles are nonaggregated, if they are not connected with large ones. Thus, 95%–98% of the small particles remain single (curve 1). The influence of an external field upon the small particle aggregation is so negligible, that corresponding curves are indistinguishable. Nevertheless the mean chain length in the bifractional model is sufficiently smaller than in the monodisperse case, our results exceed those of computer simulations in Ref. [4]. It is the consequence of the cluster definition. The fact is, no universal criteria exists for the particles to be connected in a chain. So, when trying to compare the computer simulation and the theoretical data only the qualitative coincidence is expected.

Hence, the microstructure of commercial ferrofluids proves to be as follows: the large part of main fractions (small particles with negligible interparticle interactions) remains nonaggregated; the majority of large particles (with low mole portions and high interaction energies) are connected in short chains with small particles at the edges (chains of the IIIrd class); the chain concentration is rather high, unlike the monodisperse case where the chains are long but their concentration is comparatively low. Although, this conception is related to the chain structures only, it does not contradict the possibility of quasispherical cluster existence. Such friable aggregates were found in recent computer simulations [20], for example. On the other hand, the thermodynamic approach used here describes the case of the dynamic equilibrium and reversible aggregation, which corresponds to the real ferrofluid parameters. While, as far as the magnetorheological suspensions and/or magnetic fluids with nonmagnetic holes are concerned, the chain growth has been shown [21] to be time dependent up to sizes limited by the experimental setup only. However, the presence of such "infinitely" elongated linear chains in commercial magnetic fluids would have been inevitably observed experimentally.

V. BIDISPERSE MODEL CHECK-UP: MAGNETIC BIREFRINGENCE EXPERIMENTS

As it has been already mentioned, magnetic fluids become optically anisotropic when subjected to a magnetic field. Light with its electric polarization parallel to the magnetic field is absorbed more (positive dichroism), and experiences a higher refractive index (positive birefringence), than light polarized perpendicular to the field. There are several phenomena that could be named as origins of birefringence [8].

(1) A field-induced effect in the particle material; it is worth saying, that the birefringence scale in this case is much smaller than the observed one.

(2) The internal optical anisotropy of the magnetic particles; however, normally it is not related to suspensions.

(3) A shape anisotropy of the particles; the first magnetic birefringence explanation was given in terms of ellipsoidal particles [5]. Still it is one of the most popular approaches to the problem, and a lot of experimental data is well described by it [10]. However, according to the way of magnetic core preparation and particle covering by solvent layer, the same ellipticity degree for every particle seems to be discussible.

(4) The anisotropy caused by the orientation of aggregates [6,7,9]. This explanation seems to be the most physically reasonable, as the presence of short chain aggregates in ferrofluids has been proved experimentally [2–4].

The common approach used in papers [6,7,9] was the following. A ferrofluid was approximated by the model monodisperse system with chain aggregates. Such model ferrofluid was regarded as a system of ellipsoids (with dielectric constant ε_2) suspended in carrier liquid (with dielectric constant ε_1). Each ellipsoid had the magnetic moment. Thus, the birefringence was caused by the orientation of ellipsoids which led to an internal optical anisotropy of the suspension. In Ref. [7] chains were approximated by the infinitely elongated ellipsoids, and the difference $\Delta n = n_\parallel - n_\perp$ between the refractive indices parallel $n_\parallel$ and perpendicular $n_\perp$ to the magnetic field (that is the birefringence) depended on the chain concentration Φ only (13):

$$n_\perp = \sqrt{\varepsilon_{11}}, \quad n_\parallel = \sqrt{\varepsilon_{33}}, \quad \varepsilon = \varepsilon_1 + \Phi V(\langle \mathbf{U}_{\theta\phi}\varepsilon_0\mathbf{U}^{\mathbf{T}}_{\theta\phi}\rangle - \varepsilon_1),$$

$$\varepsilon_0 = \begin{pmatrix} \dfrac{2\varepsilon_1\varepsilon_2}{\varepsilon_1+\varepsilon_2} & 0 & 0 \\ 0 & \dfrac{2\varepsilon_1\varepsilon_2}{\varepsilon_1+\varepsilon_2} & 0 \\ 0 & 0 & \varepsilon_2 \end{pmatrix}. \tag{13}$$

Here ε_{11},ε_{33} are the corresponding components of the dielectric tensor ε, the latter is to be found from the Maxwell equations. The angle brackets mean the averaging with respect to θ,ϕ, which are the angles in a cylindrical coordinate system with rotational matrix $\mathbf{U}_{\theta\phi}$ (see, Refs. [7,14]). The variable V denotes a mean chain volume.

In Ref. [9] the ellipsoid length distribution was additionally taken into account, in other words, chains were approximated by different ellipsoids. As it was mentioned earlier the mean chain length in any monodisperse model was sufficiently larger than in a bidisperse system. To check if the bidisperse model is applicable for the birefringence description, the following generalization of the earlier developed approach is used. The model ferrofluid is approximated by the carrier liquid, chains of three main classes, nonaggregated small, and large spherical particles, the corresponding concentrations of which are to be calculated from the chain distribution. The chains are replaced by elongated ellipsoids of revolution with demagnetization factors $n_i^\parallel, n_i^\perp$ parallel and perpendicular to the ellipsoid major axis respectively. Thus, the modified expression for Δn [for the original see Ref. [9] and Eq. (13)] has the following form (14):

$$\varepsilon = \varepsilon_1 + \sum_{n+m\geqslant 1}^{\infty} \sum_{i=I,II,III} g(i,n,m) V_i(\langle \mathbf{U}_{\theta\phi}\varepsilon_0\mathbf{U}^{\mathbf{T}}_{\theta\phi}\rangle - \varepsilon_1), \tag{14}$$

where $V_I = nv_2, V_{II} = nv_2 + v_1, V_{III} = nv_2 + 2v_1$ are the volumes of the Ist, IInd, and IIIrd class chains. It should be pointed out that the chain distribution $g(i,n,m)$ is the function of a magnetic field strength. So, to calculate the dielectric tensor ε for the arbitrary values of magnetic field one has to take into account not only the chain orientation but also their lengthening. As it has been already mentioned, this problem remains unsolved unfortunately. But, when an applied field is weak, the chain lengthening is negligible, and the internal optical anisotropy is in overwhelming part caused by the orientation of short and relatively stiff chains. The chain distribution obtained for zero field (11) totally meets the earlier listed requirements as three main chain classes are composed by large particles in majority, and the chains are short. Thus,

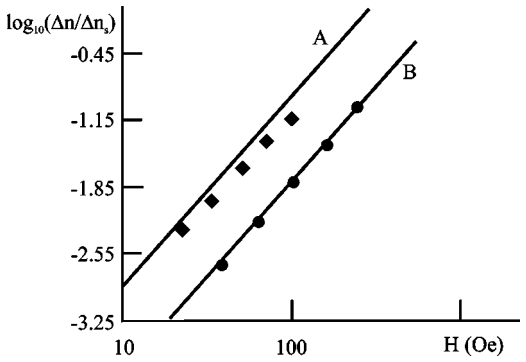

FIG. 6. Reduced birefringence $\Delta n/n_s$ as a function of applied magnetic field in log-log scale, $\Delta n_s = 8.8\times 10^{-4}$ is the birefringence saturation value. Experimental data (see Ref. [8]) for samples A and B is plotted in dots. Curves are the results of Eq. (15).

for a weak external magnetic field the tensor components from expression (14) transforms into

$$\log_{10}(\Delta n) = 2\,\log_{10}\mathbf{H} + \log_{10}\frac{\sqrt{\varepsilon_1}\varepsilon_2}{30} \times\left\{\sum_{n=2}^{\infty} V_I g(I,n,0)\alpha_I^2(n)\beta_I(n) + \sum_{n=1}^{\infty}\left[V_{II}g(II,n,1)\alpha_{II}^2(n)\beta_{II}(n) + V_{III}g(III,n,2)\alpha_{III}^2(n)\beta_{III}(n)\right]\right\}$$

$$\alpha_I = \frac{nm_2}{kT}, \quad \alpha_{II} = \frac{nm_2+m_1}{kT}, \quad \alpha_{III} = \frac{nm_2+2m_1}{kT}. \tag{15}$$

Here the values of α_i for $i=I,II,III$ are the ith class chain magnetic moments related to the thermal energy, and the coefficients β_i are defined as follows:

$$\beta_i = \beta_i^\parallel - \beta_i^\perp, \quad \beta_i^{\parallel,\perp} = \frac{1}{n_i^{\parallel,\perp}(\varepsilon_2-\varepsilon_1)+\varepsilon_1}.$$

The dependence of the magnetic birefringence (15) as a function of applied magnetic field is plotted in Fig. 6 in log-log scale. The calculations presented here were made for ferrofluids A and B from Table I. As it could be seen, the agreement with the experimental data in the weak field limit is fine. This encouraging fact verifies the chain orientation decisive influence upon the internal optical anisotropy, on the one hand. On the other, it makes us believe that the present model is applicable for a description of the magnetic birefringence as well as of the ferrofluid microstructure. As for the more general field conditions, the chain distribution obtained in Sec. III gives the 15%–20% relative increase of the mean chain length under the influence of an infinitely strengthened external field. This conclusion is in a good agreement of the experimentally observed saturation in magnetic birefringence. The latter seems to be impossible if the long linear chains are there in the system.

VI. CONCLUSION

In conclusion, the analysis presented shows that unlike the monodisperse case the model bidisperse system is weakly aggregated even at high values of the interaction energies, external magnetic field, and volume concentrations. It is the consequence of an extremely weak dipole-dipole interaction between small particles, low (not to say, very low) large particle mole portion and the poisoning effect described earlier. The comparison with computer bidisperse simulations provides a good agreement in the relative decrease of the mean chain length. The built phase diagram allows one to find the most probable chain structure in a real ferrofluid: it is the one, consisting of several large particles in the middle of a chain, at both edges of which there is one small particle. Let us stress that the phase point, corresponding to the model bidisperse fluid from Ref. [4], is situated in the region of the Ist class prevalence. This prediction meets the simulation result on the mean number of small particles per chain. Although, the major part of the large particle fraction is proved to be connected in chains, its low concentration does not permit chains to become long. More than that, the 95%–98% of small particles remain nonaggregated. Thus, the mean chain length turns out to be comparatively small (less than five particles per chain even under the influence of an external magnetic field).

The magnetic birefringence in a bidisperse model is studied theoretically for several ferrofluids in a weak field limit. The theoretical models described in Refs. [7,9] are generalized for a bifractional case. The weak field asymptotics allows to study the refractive indices difference as the function of an applied magnetic field and zero field chain distribution. The theoretical results turn out to be quite close to the ones of the experiment. It is worth mentioning that the birefringence explanation in terms of short stiff chains, under the condition when the polydispersity is taken into account, seems to be the most close to life one. Moreover, our quantitative results totally meet the experimental data obtained by Pshenichnikov *et al.* [12], according to whom: "… The most probable shape of such aggregates is a short stiff chain, formed by several large particles … No aggregates in the form of long chains have been observed …."

ACKNOWLEDGMENTS

The present research was carried out with the financial support of RFBR Grant Nos. DFG 03-02-04001 and 04-02-16078, INTAS Grant No. 03-51-6064, and RME Grant No. A03-2.9-656. The research was also made possible in part by CRDF Award No. REC-005 (EK-005-X1). In addition, the authors are greatly thankful to Professor Yu. L. Raikher for providing data and for fruitful discussions and they would like to express their gratitude to Dr. Christian Holm and Dr. Zuowei Wang for the simulation data given.

[1] D. Wei and G. N. Patey, Phys. Rev. Lett. **68**, 2043 (1992); J. J. Weis and D. Levesque, *ibid.* **71**, 2729 (1993).
[2] M. E. van Leeuwen and B. Smit, Phys. Rev. Lett. **71**, 3991 (1993); A. Satoh *et al.*, J. Colloid Interface Sci. **178**, 620 (1996); G. N. Coverdale *et al.*, J. Magn. Magn. Mater. **188**, 41 (1998); Ph. J. Camp and G. N. Patey, Phys. Rev. E **62**, 5403 (2000); A. F. Pshenichnikov and V. V. Mekhonoshin, J. Magn. Magn. Mater. **213**, 357 (2000); Z. Wang, C. Holm, and H. W. Müller, Phys. Rev. E **66**, 021405 (2002); T. Kristóf and I. Szalai, *ibid.* **68**, 041109 (2003); T. Kruse, A. Spanoudaki, and R. Pelster, Phys. Rev. B **68**, 054208 (2003).
[3] M. J. Stevens and G. S. Grest, Phys. Rev. E **51**, 5962 (1995).
[4] Z. Wang and C. Holm, Phys. Rev. E **68**, 041401 (2003).
[5] Yu. N. Skibin, V. V. Chekanov, and Yu. L. Raikher, Sov. Phys. JETP **45**, 496 (1977).
[6] P. C. Scholten, IEEE Trans. Magn. **16**, 221 (1980).
[7] S. Taketomi, Jpn. J. Appl. Phys., Part 1 **1137**, 22 (1983).
[8] E. Hasmonay *et al.*, Eur. Phys. J. B **5**, 859 (1998).
[9] M. Rasa, J. Magn. Magn. Mater. **201**, 170 (1999).
[10] A. F. Pshenichnikov and V. M. Buzhmakov, Colloid J. **63**, 305 (2001); E. Hasmonay *et al.*, J. Appl. Phys. **88**, 6628 (2000).
[11] S. Odenbach and H. Gilly, J. Magn. Magn. Mater. **152**, 123 (1996); S. Odenbach and H. Stork, *ibid.* **183**, 188 (1998); S. Odenbach, *Magnetoviscous Effects in Ferrofluids, Lecture Notes in Physics* (Springer-Verlag, Berlin, 2002).
[12] S. Kamiyama and A. Satoh, J. Colloid Interface Sci. **127**, 173 (1989); R. Rosman, J. S. M. Janssen, and M. Th. Rekveldt, J. Magn. Magn. Mater. **85**, 97 (1990); H. D. Williams, K. O'Grady, and S. W. Charles, *ibid.* **122**, 134 (1993); V. M. Buzmakov and A. F. Pshenichnikov, J. Colloid Interface Sci. **182**, 63 (1996).
[13] A. F. Pshenichnikov and I. Yu. Shurubor, Bull. Acad. Sci. USSR, Phys. Ser. (Engl. Transl.) **51**, 40 (1987); J.-C. Bacri *et al.*, J. Colloid Interface Sci. **132**, 43 (1989); H. Mamiya, I. Nakatani, and T. Furubayashi, Phys. Rev. Lett. **84**, 6106 (2000).
[14] P. Jordan, Mol. Phys. **25**, 961 (1973); **38**, 769 (1979).
[15] P. G. de Gennes and P. Pincus, Phys. Kondens. Mater. **11**, 189 (1970).
[16] A. Yu. Zubarev and L. Yu. Iskakova, J. Exp. Theor. Phys. **80**, 857 (1995); R. P. Sear, Phys. Rev. Lett. **76**, 2310 (1996); R. van Roij, *ibid.* **76**, 3348 (1996); M. A. Osipov, P. I. C. Teixeira, and M. M. Telo da Gama, Phys. Rev. E **54**, 2597 (1996); J. M. Tavares, J. J. Weis, and M. M. Telo da Gama, *ibid.* **59**, 4388 (1999); K. I. Morozov and M. I. Shliomis, in *Ferrofluids, Magnetically Controllable Fluids and Their Applications, Lecture Notes in Physics*, edited by S. Odenbach (Springer-Verlag, Berlin, 2002).
[17] A. Yu. Zubarev, J. Exp. Theor. Phys. **93**, 80 (2001).
[18] S. Kantorovich, J. Magn. Magn. Mater. **258–259**, 471 (2003);

A. O. Ivanov and S. Kantorovich, Colloid J. **65**, 166 (2003).
[19] A. O. Ivanov, J. Magn. Magn. Mater. **66**, 154 (1996).
[20] A. F. Pshenichnikov and V. V. Mekhonoshin, JETP Lett. **72**, 182 (2000); Eur. Phys. J. E **6**, 399 (2001).
[21] S. Miyazima, P. Meakin, and F. Family, Phys. Rev. A **36**, 1421 (1987); S. Fraden, A. J. Hurd, and R. B. Meyer, Phys. Rev. Lett. **63**, 2373 (1989); M. C. Miguel and R. Pastor-Satorras, Phys. Rev. E **59**, 826 (1999).